Regulation of a heterodimeric kinesin-2 through an unprocessive motor domain that is turned processive by its partner

Melanie Brunnbauer[a], Felix Mueller-Planitz[b], Süleyman Kösem[c], Thi Hieu Ho[c], Renate Dombi[c], J. Christof M. Gebhardt[a], Matthias Rief[a], and Zeynep Ökten[c,1]

[a]Physik Department E22, Technische Universität München, James-Franck-Strasse, D-85748 Garching, Germany, and Center for Integrated Protein Science Munich; [b]Adolf-Butenandt-Institut, Ludwig-Maximilians-Universität München, Schillerstrasse 44, D-80336 Munich, Germany, and Center for Integrated Protein Science Munich; [c]Institute for Cell Biology, Ludwig-Maximilians-Universität München, Schillerstrasse 42, D-80336 Munich, Germany, and Center for Integrated Protein Science Munich

Communicated by Gottfried Schatz, University of Basel, Reinach, Switzerland, April 18, 2010 (received for review March 1, 2010)

Cilia are microtubule-based protrusions of the plasma membrane found on most eukaryotic cells. Their assembly is mediated through the conserved intraflagellar transport mechanism. One class of motor proteins involved in intraflagellar transport, kinesin-2, is unique among kinesin motors in that some of its members are composed of two distinct polypeptides. However, the biological reason for heterodimerization has remained elusive. Here we provide several interdependent reasons for the heterodimerization of the kinesin-2 motor KLP11/KLP20 of *Caenorhabditis elegans* cilia. One motor domain is unprocessive as a homodimer, but heterodimerization with a processive partner generates processivity. The "unprocessive" subunit is kept in this partnership as it mediates an asymmetric autoregulation of the motor activity. Finally, heterodimerization is necessary to bind KAP1, the in vivo link between motor and cargo.

molecular motors | optical tweezers | single molecule

Molecular motors that transport cargo unidirectionally on microtubules or actin filaments over long distances without dissociating are termed processive. Paradigms of processive motors are actin-associated myosin V and microtubule-associated conventional kinesin-1 (1, 2). Both are homodimeric molecules in which two N-terminal motor domains (usually referred to as head domains) are linked via an extended C-terminal coiled-coil region. According to a generally accepted tenet, movement of single motors for hundreds of consecutive steps indeed requires such dimerization of two motor domains. Two main features emerged over the past decades to explain processivity of homodimeric motors. First, each motor domain remains strongly bound to its track for at least half of its ATPase cycle (3, 4). Second, the two identical heads of the dimer are thought to keep their ATPase cycles out of phase via a strain-dependent communication to prevent both heads from dissociating simultaneously from the track (3, 4).

The kinesin-2 family of molecular motors presents an interesting case because in addition to canonical homodimeric members, some are composed of two nonidentical heavy chains, forming heterodimers (5). Many of the representatives in the kinesin-2 family are involved in a highly conserved transport mechanism, termed intraflagellar transport (IFT) that is almost universally responsible for the formation and maintenance of cilia and flagella in eukaryotes (6). Materials destined for the ciliary tip are assembled at the base of the cilium into large rafts, which are moved to the tip by kinesin-2. Retrograde transport toward the base is powered in a similar fashion by dynein (7, 8).

In the *Caenorhabditis elegans* sensory cilium, the kinesin-like protein 11 (KLP11) and kinesin-like protein 20 (KLP20) heterodimerize to comprise a molecular motor with two distinct N-terminal catalytic motor domains (9–11). A third protein, termed kinesin-associated protein 1 (KAP1), is thought to provide the physical link between the C terminus of the heterodimeric motor protein and the IFT particle (12). The KAP1 subunit has no effects on the motor's kinetic properties (13). Interest in the ciliary transport mechanism has surged since the discovery that defects in IFT are linked to a wide range of human diseases such as Bardet–Biedl syndrome and polycystic kidney disease (14, 15).

Kinesin-2 apparently coevolved with the ciliary machinery (16, 17). However, the evolutionary advantage of combining two different motor proteins is not yet fully understood. Moreover, depending on their origin, heteromeric kinesins seem to differ dramatically in their kinetic behavior; e.g., the ciliary sea urchin kinesin-2 is an unprocessive motor, whereas in the mouse kinesin-2 (a motor that is no longer confined only to cilia but is also found in the cytoplasm) both head domains are processive as shown with homodimeric chimeras (18, 19).

Here we mechanistically dissect the *C. elegans* ciliary motor protein KLP11/KLP20 using biochemical and single-molecule assays. We present insight into the fundamental mechanistic properties of KLP11/KLP20 and provide a biological rationale for heterodimerization. We identify a motif in the KLP11/KLP20 tail that when mutated leads to a constitutively active motor in vitro. This autoinhibitory switch functions only when the motor heads are in their correct wild-type positions. We demonstrate that to obtain the heterotrimeric KLP11/KLP20/KAP1 complex that forms in vivo, the two distinct motor subunits need to be present; neither the KLP11 nor the KLP20 polypeptide chain alone bind the KAP1 subunit in vitro. The most intriguing finding, however, is that one of the motors is mechanically unprocessive as a "homodimer." Remarkably, the same subunit yields a robustly processive motor when dimerized with its partner. The KLP11/KLP20 heterodimeric kinesin-2 thus extends prior models of processivity that were based solely on studies of native homodimeric motor proteins.

Results

Overview of Constructs and Experimental Methods. We have generated a series of constructs to disentangle the kinetic properties of the individual KLP11 and KLP20 polypeptide chains within the KLP11/KLP20 heterodimer and to ultimately provide a biological rationale for the heterodimerization in *C. elegans* kinesin-2. Fig. 1 summarizes the design of the constructs and gives an overview of the experiments these constructs were subjected to. Most kinesins are autoinhibited by their C-terminal tail domain, which folds

Author contributions: Z.Ö. designed research; M.B., F.M.-P., S.K., T.H.H., R.D., J.C.M.G., and Z.Ö. performed research; F.M.-P. contributed new reagents/analytic tools; M.B., F.M.-P., S.K., and Z.Ö. analyzed data; and M.B., F.M.-P., M.R., and Z.Ö. wrote the paper.

The authors declare no conflict of interest.

[1]To whom correspondence should be addressed. E-mail: zoekten@ph.tum.de.

This article contains supporting information online at www.pnas.org/lookup/suppl/doi:10.1073/pnas.1005177107/-/DCSupplemental.

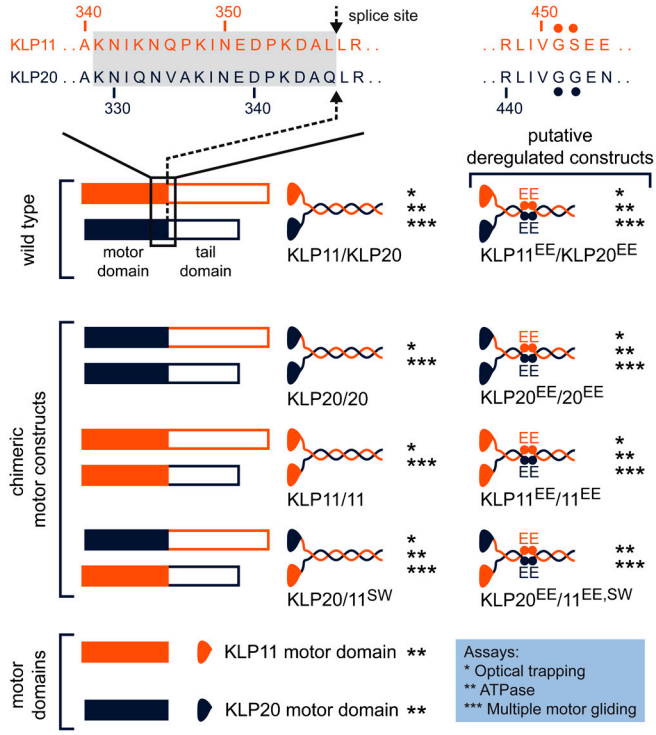

Fig. 1. Overview of constructs and assays used in this study. (*Left Top*) Shows the splice site after the neck linker (gray) used to create the chimeric constructs. The head domains in the wild-type construct were exchanged either to pair two identical heads (KLP20/20 or KLP11/11) or to swap their relative positions (KLP20/11^{SW}). The tail domains in KLP11 and KLP20 polypeptide chains were removed to contrast the enzymatic activities of the isolated motor domains (*Left Bottom*). (*Right Top*) Illustrates the sites where the point mutations were introduced to target the putative kink position in the wild-type KLP11/KLP20 protein. All chimeric constructs were expressed with these corresponding mutations as well. The asterisks assign the constructs to their designated bulk- and single-molecule assays.

back onto the catalytic heads. This autoinhibition can be relieved by introducing point mutations in the so-called kink region of the tail domain. To probe for the presence of such an autoregulatory mechanism in KLP11/KLP20, we introduced mutations in the tail domains of the KLP11 and the KLP20 polypeptide chains (20). Moreover, we designed chimeras with splice sites between the head and the tail domains (18), resulting in heterodimeric constructs with identical head domains, or constructs whose head domains are swapped compared to the wild type. These chimeras allowed us to dissect the significance of KLP11 and KLP20 for autoinhibition and processivity in *C. elegans* kinesin-2.

***C. elegans* KLP11/KLP20 Is a Processive Motor.** We first assessed whether KLP11/KLP20 is capable of moving processively along microtubules. We employed two single-molecule assays, one capable of detecting processive movement at saturating ATP and one at subsaturating ATP concentrations. In the former assay, motors are attached to polystyrene beads, and the fraction of moving beads is determined as a function of motor-to-bead ratio in an optical trap. Briefly, polystyrene beads coated with decreasing amounts of motors are trapped in a focused laser beam and maneuvered close to surface-attached microtubules (Fig. 2*A Left*). Motors on the bead surface bind to the microtubule track, move the bead out of the trap focus, and are repeatedly pulled back into focus when the motor releases from its track. Such movements are generally referred to as "walking" events. At single-molecule level, the number of such walks in a defined time frame provides a direct readout on the motor's activity and is henceforth termed "single-molecule walking frequency" (SMWF) (Fig. 2*A Left*).

The fraction of moving beads as a function of motor density is fit to a Poisson distribution to determine if a single motor protein is sufficient to move the bead (2). Fig. 2*B* demonstrates that motor activity of wild-type KLP11/KLP20 is best fit to a model in which bead motility is the result of the activity of a single kinesin molecule, providing strong evidence for processivity. In the second single-molecule assay, we tested processivity at subsaturating ATP concentrations. With subsaturating ATP, the consecutive stepping of a processive motor is sufficiently slow to be directly visualized with nanometer precision using an optical trap (Fig. 2*A Right*). In the single-molecule regime, i.e., at limiting motor-to-bead ratios, multiple steps of 8 nm were revealed, providing direct proof for processive motion of the wild-type KLP11/KLP20 heterodimer (Fig. 2*C*).

KLP11/KLP20 Is Autoinhibited by Its Tail Domain. Collection of the data described above proved to be difficult due to the low SMWFs displayed by the wild-type KLP11/KLP20 motor. We hypothesized that this might be due to autoinhibitory folding of the tail domain onto the motor domain. A number of kinesins use regulatory folding in the so-called kink region to prevent futile ATP hydrolysis (20–24). This autoinhibition is thought to be relieved when the tail domain of the motor binds to its cargo in vivo or in vitro (20, 25–28). Cargo binding most likely causes a large conformational change in the molecule leading to a more extended conformation. Such folded and extended conformations of the heterodimeric sea urchin ciliary kinesin-2 and other kinesin molecules have been directly visualized in electron micrographs (29–31). This tail inhibition can be prevented by introducing mutations in the kink that presumably force formation of an extended coiled coil, as shown for the kinesin-1 motors or the homodimeric Osm3, the partner kinesin-2 motor of *C. elegans* (20, 32, 33). Coiled-coil prediction programs indeed detect a discontinuity in the probability to form a coiled coil at a location in the KLP11/KLP20 proteins analogous to that of the Osm3 motor (34). We therefore introduced mutations aimed at generating continuous coiled coils in both KLP11 and KLP20 (G451E, S452E for KLP11, and G444E, G445E for KLP20). The resulting construct, designated KLP11^{EE}/KLP20^{EE}, demonstrates a dramatic increase in SMWF compared to the wild-type KLP11/KLP20 motor (Fig. 2*D*). As the wild-type KLP11/KLP20 protein, KLP11^{EE}/KLP20^{EE} moves processively on microtubules (Fig. S1). We conclude that the wild-type KLP11/KLP20 protein is autoinhibited and that mutations at the kink relieve autoinhibition.

KLP11/KLP20 Is Not a Conspicuous Limper. The KLP11/KLP20 protein combines two different polypeptide chains to one double-headed motor. If one subunit were a significantly faster motor than the other, one might expect that the motor "limps." Such limping would become evident from alternating short and long dwells between steps. The single-molecule stepping traces did not reveal any conspicuous limping of the KLP11 and KLP20 motor domain combinations (Fig. S2*A*). A quantitative analysis confirmed this notion. We quantified the observed degree of limping from the dwell times as previously described and compared the measured degree of limping in our traces with a dataset obtained from simulated stepping traces (35). The quantitative treatment of the stepping traces of KLP11 and KLP20 is consistent with no or only a modest amount of limping. The analysis provides an upper limit of a factor of 2 to 3 for the difference in the stepping rates. This contrasts with an artificial kinesin-1 heterodimer displaying a limping factor of at least 10 caused by a point mutation in one catalytic head (36). Notably, the corresponding homodimeric kinesin-1 with both heads containing the point mutation was unprocessive. The small limping factor of KLP11/KLP20 indicates that neither subunit is an exceptionally faster motor subunit.

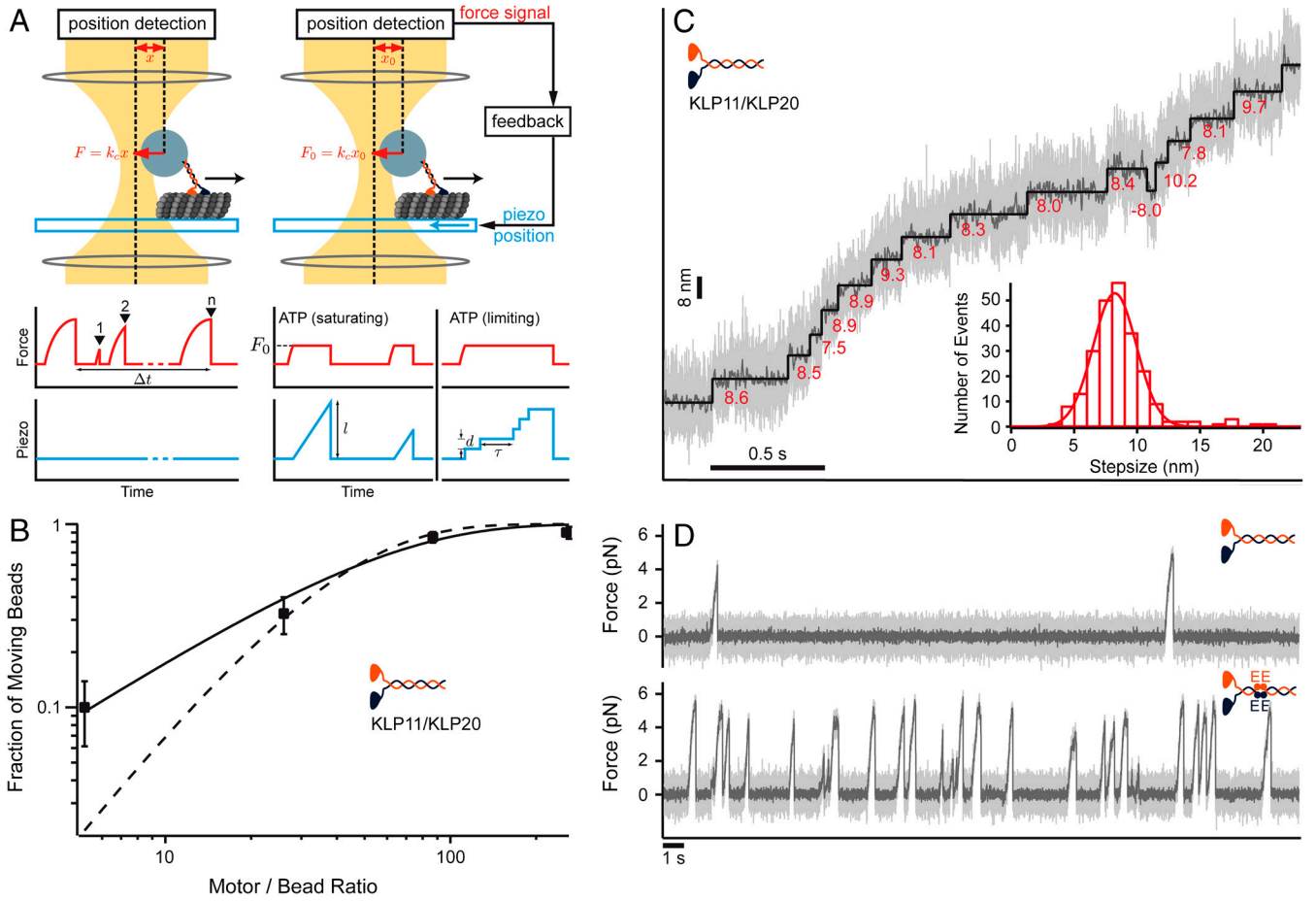

Fig. 2. The KLP11/KLP20 heterodimer is an autoinhibited and processive molecular motor. (*A*) Schematics of the experimental setup. (*Left*) Stationary trapping of a polystyrene bead (blue) that is decorated with motor proteins in a focused laser beam (yellow). The optical trap exerts a force on the bead that can be approximated by Hooke's Law ($F = k_c x$), where k_c is the spring constant of the laser trap and x is the displacement of the bead. The red curve illustrates "walking events" displayed by a single motor attached to a trapped bead. The number of such "walks" per time frame defines the SMWF of a motor and thus a measure for its motor activity. (*Right*) Force feed-backed trapping mode. The restoring force acting on the motor is clamped to a constant value F_0 by moving the piezo stage in the opposite direction to the motor's movement. Contrary to the stationary modus, the piezo signal (light blue) gives information about the run length (l) of a motor and allows resolving discrete steps (step size d, dwell time τ) at limiting ATP concentrations. (*B*) A single KLP11/KLP20 molecule can support bead movement. The fraction of moving beads at saturating ATP concentrations (2 mM) is plotted against the calculated number of KLP11/KLP20 molecules per bead and fit to models that require only one [solid line: $f(x) = 1 - \exp(-\lambda * x)$] or minimally two motors to move a bead [dashed line: $f(x) = 1 - \exp(-\lambda * x) - \lambda * x * \exp(-\lambda * x)$]. (*C*) Resolving individual steps of a single KLP11/KLP20 molecule at subsaturating ATP (5 μM) under constant backward load (1.4 pN). Raw data: light gray, box-filtered data: dark gray. An automated step finder identified the step sizes (red numbers) of individual steps of a single KLP11/KLP20 molecule (black line). (*Inset*) histogram of step sizes. The Gaussian fit reveals a step size of (8.23 ± 0.16) nm (mean ± SEM) ($N = 239$). (*D*) Mutations in the tail domain of KLP11/KLP20 increase the frequency with which a single motor initiates a processive run.

The occurrence of moderate limping in some traces could be indicative of a residual kinetic difference between the subunits or simply point to an artifact introduced by the assay. Limping has in fact been observed also for conventional, homodimeric kinesin-1. The degree of limping was strongly affected by the magnitude of the vertical force acting on the motor and was influenced, e.g., by the length of the stalk (37). In our assays, motors are unspecifically attached to beads. We suspect that traces displaying a moderate degree of limping possibly result from motors that are attached to the beads with a longer portion of their stalks.

Dissection of KLP11/KLP20's Processivity. The question why nature combined two different polypeptide chains to create a heterodimeric motor specifically for ciliary function early in the evolution is intriguing (16, 17). To dissect the contribution of the individual heads to the overall processivity in the wild-type KLP11/KLP20 motor, we expressed chimeras containing two identical heads. As judged by native size-exclusion chromatography, neither KLP11 nor KLP20 polypeptide chains are capable of forming homodimers. Two KLP11 heads or two KLP20 heads along with their native neck linkers were therefore fused to the heterodimeric tail (Fig. 1), which ensures reliable dimerization (9). We designated these chimeric constructs as KLP11/11 or KLP20/20 to stress the presence of two identical heads. To test if these constructs are autoinhibited, both wild-type and constitutively active heterodimeric tails were used. We also generated a double-chimeric motor in which the head domains were swapped (henceforth termed KLP20/11^{sw}) to determine if domain swapping had deleterious effects per se (Fig. 1).

We first assessed whether the chimeric constructs retained the ability to move beads in a processive fashion. KLP20/20 chimera indeed showed processive movement (Fig. S3*A*) and single molecules displayed multiple 8-nm steps under subsaturating ATP conditions (Fig. 3*A*). However, although capable of moving beads at saturating ATP concentrations and high motor-to-bead ratios, the KLP11/11 chimera with the wild-type tail was unable to support processive movement at limiting motor-to-bead ratios (Fig. 3*B* and Fig. S4). This contrasts with equivalent constructs

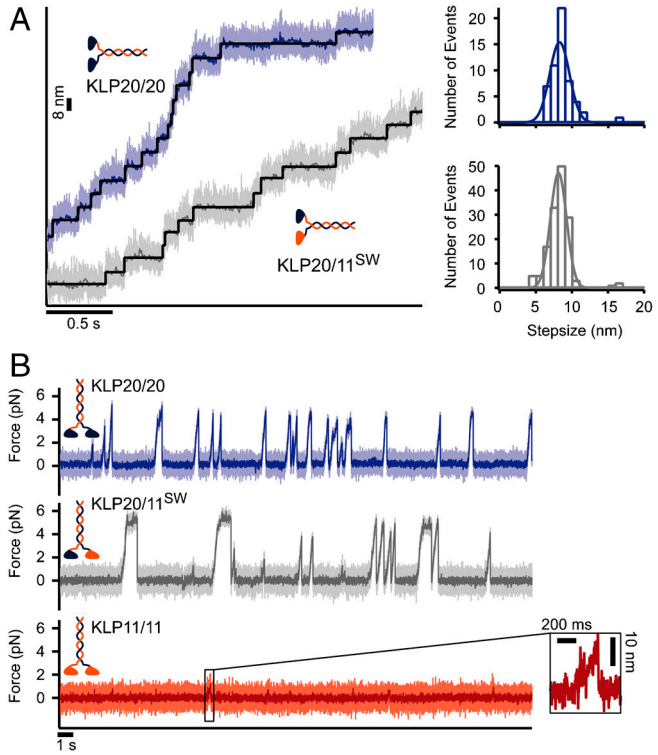

Fig. 3. Two KLP11 motor domains paired with each other cannot coordinate to support processive stepping. (*A*) The KLP20/20 chimera (*Upper Trace*) and the double-chimeric KLP20/11^{sw} (*Lower Trace*) take multiple steps at subsaturating ATP. Gaussian fits to step size histograms reveal an (8.28 ± 0.26) nm (mean $\pm$ SEM) step size for KLP20/20 ($N = 55$) and (8.14 ± 0.13) nm (mean$\pm$ SEM) for KLP20/11^{sw} ($N = 145$). (*B*) Also at saturating ATP (2 mM) single molecules of KLP20/20 (blue) and KLP20/11^{sw} (gray) initiate processive runs in stark contrast to the KLP11/11 chimera (red) which only rarely generated a detectable signal. Note that the junction between the KLP11 head and the KLP20 tail domain in the chimera is functional as the double-chimeric protein KLP20/11^{sw} shows robust processivity.

of mouse kinesin-2 where the homodimers are reported to be processive (18). Importantly, also the constitutively active KLP11^{EE}/11^{EE} chimera did not show signs of processive movement ruling out the possibility that KLP11/11 is simply autoinhibited by its wild-type tail (Fig. S4).

In principle, fusion of the KLP11 head to the KLP20 tail domain could yield a nonfunctional junction in the KLP11/11 chimera. The KLP20/11^{sw} double chimera contains the same chimeric polypeptide chain with the identical junction and thus allows us to directly test that possibility. We have probed the activity of this double chimera at the multiple-motor level using gliding assays and at the single-motor level in the optical trap. In gliding assays, surface-attached kinesins move fluorescently labeled microtubule filaments in an ATP-dependent manner. Active motors on the surface propel microtubule filaments continuously and smoothly, without any interruptions in their movement. Such assays allow the determination and quantitative comparison of motors' velocities at multiple-motor level. The observed velocities of multiple KLP20/11^{sw} motors were quantitatively similar to those of wild-type KLP11/KLP20 and both motors displayed robust gliding of microtubule filaments (Fig. S5 and Movies S1–S4), providing evidence for the integrity of the chosen junction. Likewise, no difference between the wild-type motor and the double chimera was discernible at the single-molecule level. Using the optical trap, we resolved consecutive 8-nm steps at limiting motor-to-bead ratios (Fig. 3*A* and Fig. S3*B*). We conclude that the transplantation of the heads has no deleterious effects per se. We excluded trivial explanations for the lack of processivity of the KLP11/11 chimera, such as protein aggregation or dissociation into monomers using size-exclusion chromatography coupled to multiple angle light scattering (MALS). All constructs were nonaggregated and had molecular weights consistent only with dimers (Fig. S6). Furthermore, all chimeras displayed robust motility in multiple-motor gliding assays revealing that the microtubule-activated ATPase of the constructs is undisturbed (Movies S3–S8). All chimeric constructs moved microtubules at wild-type velocities except the KLP11/11 chimera, which displayed half of the wild-type velocity (Fig. S5). In summary, all constructs are active dimers, and both the KLP20/20 chimera and the KLP20/11^{sw} double chimera are processive, whereas KLP11/11 is not.

Does the KLP11 Subunit Shorten the Processive Run Length of the KLP20 Subunit? We directly contrasted the single-molecule run length distributions of the KLP20^{EE}/20^{EE} chimera and the KLP11^{EE}/KLP20^{EE} to assess if the presence of the unprocessive KLP11 subunit curtails the length of the processive runs of the KLP20 subunit. Both motors are equivalent in the average distance they travel on the microtubule filament, providing further evidence that the KLP11 subunit fully supports processive stepping when paired with the KLP20 subunit (Fig. 4).

Kinetic Properties of the KLP11 and KLP20 Heads. The gliding filament assays demonstrate that the combination of two KLP11 heads yields a slow motor. In contrast, all other head domain combinations move microtubules at wild-type velocities (Fig. S5). To test if the kinetic differences are inherent to the respective heads or arise from dimerization, we further dissected the kinetic properties of the dimeric full-length constructs along with monomeric head domains (including their respective neck linkers) in microtubule-activated ATPase assays. The steady-state kinetic properties of the isolated monomeric head domains are equivalent in their microtubule-binding properties (K_M) and their maximum ATP hydrolysis rates (k_{cat}) (Fig. S7*A*). The kinetic equivalence of the free head domains is significant as it demonstrates that the unconstrained KLP11 head domain is capable of turning over ATP at speeds similar to the unconstrained KLP20

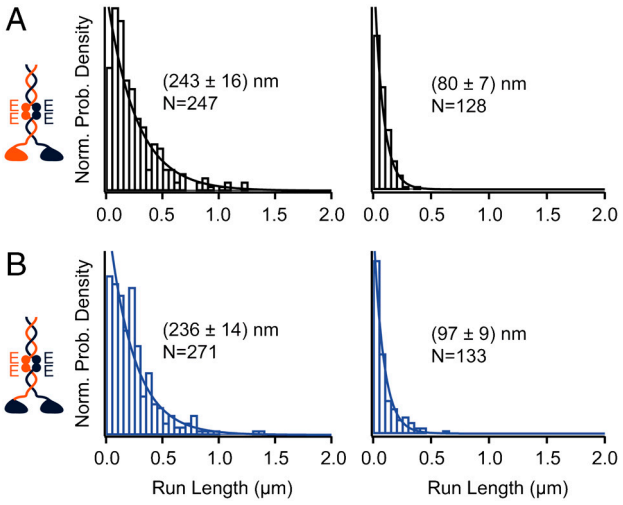

Fig. 4. Run-length distributions of the KLP11 and KLP20 vs. the KLP20 and KLP20 head combination under constant force. At single-molecule level, run lengths of the KLP11^{EE}/KLP20^{EE} (*A*) and the KLP20^{EE}/20^{EE} (*B*) motors were measured at low (*Left*, 2 pN and 1.7 pN, respectively) and at high forces (*Right*, 4 pN and 3.7 pN, respectively) under saturating ATP conditions (2 mM). Values are average run lengths ($\pm$SEM). Despite the presence of an unprocessive KLP11 subunit, the average run length of the KLP11 and KLP20 head domain combination is equivalent to the combination of two KLP20 head domains.

head. To interrogate the effects of dimerization on the ATP turnover, we assayed all possible combinations of these head domains in the context of the full-length protein. To avoid artifacts caused by autoinhibition, we assayed all full-length constructs in the context of the constitutively active tail domains to obtain the maximum hydrolysis rates possible. All constructs hydrolyzed ATP at similar rates with the exception of KLP11^{EE}/11^{EE} whose maximum ATP turnover rate was approximately three times lower (Fig. S7*B*). The steady-state turnover rates thus demonstrate that it is the combination of two KLP11 heads that leads to a suppressed ATPase activity, which is then relieved if KLP11 is combined with the KLP20 head. It is particularly noteworthy that the double chimera KLP20^{EE}/11^{EE,sw}, in which the head domains are swapped, and the KLP11^{EE}/11^{EE} chimera have distinct enzymatic activities although the same "slow" subunit (the KLP11 head fused to the KLP20^{EE} tail) is present in both. In the KLP20^{EE}/11^{EE,sw}, this subunit does not curtail the ATPase activity but indeed fully supports the enzymatic activity at wild-type levels (Fig. S7*B*). This behavior bears qualitative resemblance to our single-molecule data, where the KLP11/11 chimera cannot support processive runs. Yet the double-chimera KLP20/11^{sw}, which contains the exact same chimeric KLP11 head/KLP20-tail polypeptide, fully supports processive stepping at wild-type levels. We conclude that even though the enzymatic properties of the motor domains alone are equivalent, KLP11 exhibits different kinetic properties in a dimeric context depending on the identity of its partner head.

Requirements for Heterotrimerization. We hypothesized that heterodimerization could be important for binding of KAP1, the protein that is proposed to physically attach the KLP11/KLP20 motor to its IFT cargo. To test this hypothesis we performed pull-down experiments with wild-type KLP11, KLP20, and KAP1 subunits. When KAP1 was coexpressed with KLP11 as well as KLP20 in insect cells using the Baculovirus expression system, the heterotrimeric complex was purified via the Flag tag at the C terminus of KLP11. To test which subunit is responsible for KAP1 binding, KAP1 was coexpressed with either KLP11 or KPL20. Immunoprecipitation of KLP11 or KLP20 via their C-terminal Flag tag demonstrated that neither polypeptide could coprecipitate KAP1 (Fig. S8*A*). The heterotrimeric complex is coprecipitated efficiently regardless of which of the three subunits is Flag tagged (Fig. S8*B*) ruling out a possible interference of the C-terminal Flag tag with the KAP1 subunit. We conclude that the presence of both polypeptide chains is essential to form the heterotrimeric KLP11/KLP20/KAP1 complex.

Requirements for Autoinhibition in KLP11/KLP20. The chimeric constructs allow us to determine whether both heads are similarly affected by autoinhibition (Fig. 2*D*) or whether the identity or the location of the heads relative to the heterodimeric tail is important. Surprisingly, the SMWFs of the homodimeric chimera KLP20/20 and the heterodimeric double-chimera KLP20/11^{sw} were indistinguishable from the constitutively active KLP11^{EE}/KLP20^{EE} motor (Figs. 5*A* and 3*B*). These data demonstrate that for autoinhibition to be effective, the KLP11 motor domain must be joined to its proper KLP11 tail, as the double-chimera KLP20/11^{sw}, where the KLP11 motor domain is present but attached to the "wrong" tail, fails to show autoinhibition. Thus regulation of the native heterodimer is asymmetric and depends on correct positioning of the KLP11 motor domain.

We tested predictions of the asymmetric inhibition model in independent microtubule-activated ATPase bulk assays. The model predicts that the ATPase activity of the wild-type protein with the wild-type tail domain free in solution is suppressed and that simply switching the heads would restore the activity. In contrast, switching the heads in the context of the constitutively active tails would be expected not to affect ATP hydrolysis

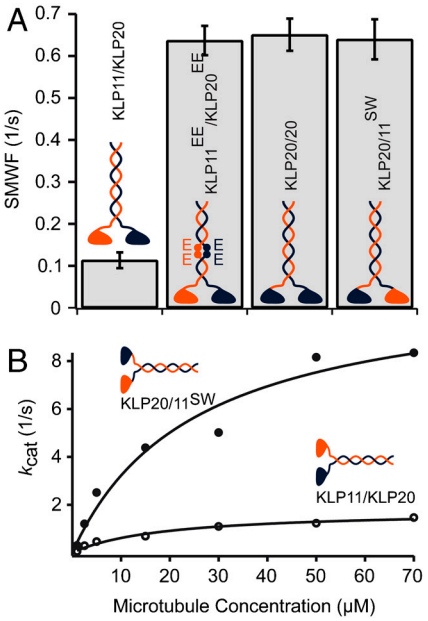

Fig. 5. (*A*) Autoinhibition by the tail domain is asymmetric and is mediated through the KLP11 head. At the single-molecule level, the autoinhibited wild-type KLP11/KLP20 displays a SMWF that is sixfold lower than the constitutively active KLP11^{EE}/KLP20^{EE} motor. The SMWFs of KLP20/20 and KLP20/11^{sw} are quantitatively the same as that of KLP11^{EE}/KLP20^{EE}, suggesting that autoinhibition is possible only if both KLP11 and KLP20 heads are present and are attached to their wild-type tails. (*B*) Switching on the motor by switching the motor domains. The suppressed ATPase of wild-type KLP11/KLP20 heterodimer is relieved in the KLP20/11^{sw} chimera with swapped head domains. As predicted from our single-molecule data, the ATPase activity of the wild-type KLP11/KLP20 is suppressed in solution (k_{cat} = 1.8 s^{-1}, K_M = 19 μM for KLP11/KLP20). Remarkably, switching the positions of the heads is sufficient to relieve this suppression (k_{cat} = 11.3 s^{-1}, K_M = 25 μM for KLP20/11^{sw}).

because these constructs are not autoinhibited. We demonstrated above that the latter prediction is met (Fig. S7*B*). Fig. 5*B* now shows that also the former prediction holds true: The suppression of the ATPase activity in the wild-type protein is relieved by merely switching the positions of the heads.

Discussion

What does it take to be processive? Our single-molecule analysis demonstrates that processivity can also be brought about by two kinetically nonequivalent polypeptide chains in nature: a motor subunit that is robustly processive when "homodimeric" (KLP20/20) paired up with a motor that is mechanically unprocessive as a "homodimer" (KLP11/11) is capable of robust processive movement by taking alternate, equivalent steps (Fig. S9*A*). This is demonstrated for both the wild-type KLP11/KLP20 heterodimer and the artificial KLP20/11^{sw} double chimera (Figs. 2*C* and 3*A*). Remarkably, in these contexts KLP11 does not behave as a "millstone around the neck" of KLP20 that curtails its activity, unlike dimeric kinesin-1 with one mutated motor domain (36). On the contrary, when paired up with KLP20, KLP11 turns into an equivalent partner that fully supports processive behavior without affecting the run lengths (Fig. 4).

Why is only the KLP11/11 chimera incapable of walking processively? So far all native homodimeric processive motors, myosins as well as kinesin, were shown to walk according to the hand-over-hand model where the positions of the two heads alternate with each step (38–41). Perhaps the KLP11 heads in the dimeric context cannot freely swing past each other due to steric reasons, or due to a direct inhibitory interaction of two KLP11 heads. Severing the heads off their tail domain would relieve this

inhibition, explaining the equivalent ATPase kinetics of the isolated KLP11 and KLP20 monomeric head domains (Fig. S7*A*). Moreover, the model would readily explain why the KLP11 head domain does not curtail the ATPase activity and processivity in the wild-type or the double-chimeric motor. A built-in cross-inhibitory feature of the KLP11 subunit might have assisted nature to evolve a heterodimeric motor.

What is the purpose of an "unprocessive" subunit in a transport motor? Our mechanistic analysis offers an explanation. First, both KLP11 and KLP20 polypeptide chains need to be present to effectively bind the KAP1 subunit, the proposed protein linker of the motor to its IFT cargo in vivo. Second, and more importantly, the wild-type KLP11/KLP20 protein combines two kinetic traits: an autoregulated but unprocessive KLP11 subunit and an unregulated but processive KLP20 subunit that come together to yield an autoregulated and processive motor protein. We suggest that it is the ability to act as a regulator that makes KLP11 indispensable. Swapping the relative positions of the motor domains abolishes this autoregulation as shown by the processive and unregulated double-chimera KLP20/11^{sw} in single molecule as well as bulk assays (Figs. 3*A* and 5). In fact, only the wild-type configuration KLP11/KLP20 yields a motor that is both processive and autoregulated (Fig. S9*B*). In building sensory cilia, the heterodimeric KLP11/KLP20 kinesin works in concert with the homodimeric Osm3 kinesin to generate and maintain the ciliary axoneme (11). Osm3 is a processive motor that also has a regulatory switch in its tail domain that presumably unfolds the tail and renders Osm3 constitutively active (20). However, transforming *C. elegans* with the constitutively active form of Osm3 displays a phenotype that is indistinguishable from the Osm3-null mutant (11). An active but deregulated Osm3 motor seems unable to perform its in vivo tasks. It is plausible that the same regulatory mechanism is crucial also for the in vivo function of the KLP11/KLP20 heterodimer.

Although the list of mechanistically scrutinized kinesin-2 motors is not extensive, this family already proved to be kinetically diverse with the sea urchin kinesin-2 being unprocessive and mouse kinesin-2 being processive (18, 19). The heterodimeric KLP11/KLP20 motor from *C. elegans* adds yet another nuance to the color spectra of the kinesin-2 family by combining a processive head with an unprocessive one to walk processively. It will be interesting to see if and which of the results presented here with the KLP11/KLP20 motor will be applicable to the ciliary kinesin-2 motors from other organisms.

Methods

All constructs were expressed using the Baculovirus expression system with a C-terminal Flag tag to facilitate protein purification. Microtubule-activated ATPase assays were preformed in the N-(2-Acetamido)-2-aminoethanesulfonic acid reaction buffer using a BioTek plate reader. All optical trapping and multiple-motor gliding experiments were performed in the standard BRB80 buffer with some modifications. Trapping experiments and motility assays were performed with a custom-built optical tweezers setup equipped with fluorescence microscopy (see *SI Text* for detailed information).

ACKNOWLEDGMENTS. We thank Jonathan M. Scholey (University of California, Davis) for his generous gift of kinesin-2 plasmids, Peter Becker (University of Munich) for the opportunity to do the MALS and ATPase assays in his laboratory, and P. Becker, M. Schleicher, and G. Woehlke for fruitful discussions and comments on the paper. This work was supported by a Long Term European Molecular Biology Organization fellowship to Z.Ö. and grants from the Deutsche Forschungsgemeinschaft (DFG) and the Friedrich-Baur-Stiftung to Z.Ö. and Manfred Schliwa. M.B. was funded by the DFG SFB486.

1. Mehta AD, et al. (1999) Myosin-V is a processive actin-based motor. *Nature* 400:590–593.
2. Block SM, Goldstein LS, Schnapp BJ (1990) Bead movement by single kinesin molecules studied with optical tweezers. *Nature* 348:348–352.
3. Cross RA (2004) The kinetic mechanism of kinesin. *Trends Biochem Sci* 29:301–309.
4. Rock Ronald S, Purcell Thomas J, Spudich James A (2003) Mechanics of unconventional myosins. *The Enzymes* 23:55–86.
5. Cole DG (1999) Kinesin-II, the heteromeric kinesin. *Cell Mol Life Sci* 56:217–226.
6. Kozminski KG, Johnson KA, Forscher P, Rosenbaum JL (1993) A motility in the eukaryotic flagellum unrelated to flagellar beating. *Proc Natl Acad Sci USA* 90:5519–5523.
7. Scholey JM (2003) Intraflagellar transport. *Annu Rev Cell Dev Biol* 19:423–443.
8. Rosenbaum JL, Witman GB (2002) Intraflagellar transport. *Nat Rev Mol Cell Biol* 3:813–825.
9. Pan X, et al. (2006) Mechanism of transport of IFT particles in C. elegans cilia by the concerted action of kinesin-II and OSM-3 motors. *J Cell Biol* 174:1035–1045.
10. Scholey JM (2008) Intraflagellar transport motors in cilia: Moving along the cell's antenna. *J Cell Biol* 180:23–29.
11. Snow JJ, et al. (2004) Two anterograde intraflagellar transport motors cooperate to build sensory cilia on C. elegans neurons. *Nat Cell Biol* 6:1109–1113.
12. Ou G, Blacque OE, Snow JJ, Leroux MR, Scholey JM (2005) Functional coordination of intraflagellar transport motors. *Nature* 436:583–587.
13. Yamazaki H, Nakata T, Okada Y, Hirokawa N (1996) Cloning and characterization of KAP3: a novel kinesin superfamily-associated protein of KIF3A/3B. *Proc Natl Acad Sci USA* 93:8443–8448.
14. Bisgrove BW, Yost HJ (2006) The roles of cilia in developmental disorders and disease. *Development* 133:4131–4143.
15. Pazour GJ, Rosenbaum JL (2002) Intraflagellar transport and cilia-dependent diseases. *Trends Cell Biol* 12:551–555.
16. Scholey JM (2003) Intraflagellar transport. *Annu Rev Cell Dev Biol* 19:423–443.
17. Mitchell DR (2007) The evolution of eukaryotic cilia and flagella as motile and sensory organelles. *Adv Exp Med Biol* 607:130–140.
18. Muthukrishnan G, Zhang Y, Shastry S, Hancock WO (2009) The processivity of kinesin-2 motors suggests diminished front-head gating. *Curr Biol* 19:442–447.
19. Pierce DW, Hom-Booher N, Otsuka AJ, Vale RD (1999) Single-molecule behavior of monomeric and heteromeric kinesins. *Biochemistry* 38:5412–5421.
20. Imanishi M, Endres NF, Gennerich A, Vale RD (2006) Autoinhibition regulates the motility of the C. elegans intraflagellar transport motor OSM-3. *J Cell Biol* 174:931–937.
21. Hackney DD, Stock MF (2000) Kinesin's IAK tail domain inhibits initial microtubule-stimulated ADP release. *Nat Cell Biol* 2:257–260.
22. Hackney DD, Stock MF (2008) Kinesin tail domains and Mg2+ directly inhibit release of ADP from head domains in the absence of microtubules. *Biochemistry* 47:7770–7778.
23. Verhey KJ, Hammond JW (2009) Traffic control: Regulation of kinesin motors. *Nat Rev Mol Cell Biol* 10:765–777.
24. Dietrich KA, et al. (2008) The kinesin-1 motor protein is regulated by a direct interaction of its head and tail. *Proc Natl Acad Sci USA* 105:8938–8943.
25. Espeut J, et al. (2008) Phosphorylation relieves autoinhibition of the kinetochore motor Cenp-E. *Mol Cell* 29:637–643.
26. Hammond JW, et al. (2009) Mammalian Kinesin-3 motors are dimeric in vivo and move by processive motility upon release of autoinhibition. *PLoS Biol* 7:e72.
27. Friedman DS, Vale RD (1999) Single-molecule analysis of kinesin motility reveals regulation by the cargo-binding tail domain. *Nat Cell Biol* 1:293–297.
28. Jiang MY, Sheetz MP (1995) Cargo-activated ATPase activity of kinesin. *Biophys J* 68:283S–284S discussion 285S.
29. Hackney DD, Levitt JD, Suhan J (1992) Kinesin undergoes a 9 S to 6 S conformational transition. *J Biol Chem* 267:8696–8701.
30. Hirokawa N, et al. (1989) Submolecular domains of bovine brain kinesin identified by electron microscopy and monoclonal antibody decoration. *Cell* 56:867–878.
31. Wedaman KP, Meyer DW, Rashid DJ, Cole DG, Scholey JM (1996) Sequence and submolecular localization of the 115-kD accessory subunit of the heterotrimeric kinesin-II (KRP85/95) complex. *J Cell Biol* 132:371–380.
32. Seiler S, et al. (2000) Cargo binding and regulatory sites in the tail of fungal conventional kinesin. *Nat Cell Biol* 2:333–338.
33. Coy DL, Hancock WO, Wagenbach M, Howard J (1999) Kinesin's tail domain is an inhibitory regulator of the motor domain. *Nat Cell Biol* 1:288–292.
34. Lupas A, Van Dyke M, Stock J (1991) Predicting coiled coils from protein sequences. *Science* 252:1162–1164.
35. Asbury CL, Fehr AN, Block SM (2003) Kinesin moves by an asymmetric hand-over-hand mechanism. *Science* 302:2130–2134.
36. Kaseda K, Higuchi H, Hirose K (2003) Alternate fast and slow stepping of a heterodimeric kinesin molecule. *Nat Cell Biol* 5:1079–1082.
37. Fehr AN, Gutierrez-Medina B, Asbury CL, Block SM (2009) On the origin of kinesin limping. *Biophys J* 97:1663–1670.
38. Yildiz A, Tomishige M, Vale RD, Selvin PR (2004) Kinesin walks hand-over-hand. *Science* 303:676–678.
39. Okten Z, Churchman LS, Rock RS, Spudich JA (2004) Myosin VI walks hand-over-hand along actin. *Nat Struct Mol Biol* 11:884–887.
40. Yildiz A, et al. (2003) Myosin V walks hand-over-hand: Single fluorophore imaging with 1.5-nm localization. *Science* 300:2061–2065.
41. Yildiz A, et al. (2004) Myosin VI steps via a hand-over-hand mechanism with its lever arm undergoing fluctuations when attached to actin. *J Biol Chem* 279:37223–37226.